

EFFECTS OF PANEL ZONE STRENGTH AND BEAM WEB CONNECTION METHOD: SEISMIC PERFORMANCE OF REDUCED BEAM SECTION STEEL MOMENT CONNECTIONS

Cheol-Ho Lee¹; Sang-Woo Jeon²; Jin-Ho Kim³; Jae-Hoon Kim⁴; Chia-Ming Uang⁵

SUMMARY

This paper presents test results on eight reduced beam section (RBS) steel moment connections. The testing program addressed bolted versus welded web connection and panel zone (PZ) strength as key variables. Specimens with medium PZ strength were designed to promote energy dissipation from both PZ and RBS regions such that the requirement for expensive doubler plates could be reduced. Both strong and medium PZ specimens with a welded web connection were able to provide satisfactory connection rotation capacity for special moment-resisting frames. Specimens with a bolted web connection performed poorly due to premature brittle fracture of the beam flange at the weld access hole. If fracture within the beam flange groove weld was avoided using quality welding, the fracture tended to move into the beam flange base metal at the weld access hole. The measured strain data showed that the classical beam theory does not provide reliable shear transfer prediction in the connection. Criteria for a balanced PZ strength that improves the plastic rotation capacity while reduces the amount of beam distortion are also proposed.

INTRODUCTION

As a response to the widespread damage in connections of steel moment-resisting frames that occurred during the 1994 Northridge, California and the 1995 Kobe, Japan earthquakes, a number of improved beam-to-column connection design strategies have been proposed. Of a variety of new designs, the reduced beam section (RBS) connection has been shown to exhibit satisfactory levels of ductility in numerous tests and has found broad acceptance in a relatively short time (Chen 1996; Plumier 1997; Zekioglu et al. 1997; Engelhardt et al. 1998). In the RBS connection a portion of the beam flanges at some distance from the column face is strategically removed to promote stable yielding at the reduced section and to effectively protect the more vulnerable welded joints. This weakening strategy also reduces the seismic force demand on the column and the panel zone. Although this type of moment connection has been widely used in the past few years, there remain several design issues that should be further examined

¹Assoc. professor, Dept. of Architecture, Seoul National Univ., Korea, Email: cheolee@snu.ac.kr

²Research Engineer, Research Institute of Science and Technology, Korea, Email: jswsy@rist.re.kr

³Research Engineer, Research Institute of Science and Technology, Korea, Email: jhkim@rist.re.kr

⁴Graduate Student, Dept. of Architecture, Seoul National Univ., Korea, Email: kaine@chol.com

⁵Professor, Dept. of Structural Engineering, Univ. of California, San Diego, USA, Email: cmu@ucsd.edu

(for example, Jones et al. 2002; Gilton and Uang 2002; Chi and Uang 2002). The primary objective of this experimental study was to investigate the effects of beam web connection type and panel zone strength on the seismic performance of RBS connections

TESTING PROGRAM

Design of Test Specimens

A total of eight full-scale test specimens were designed and grouped as Set No. 1 and Set No. 2 (Table 1). Typical geometry and seismic moment profile for the design of the radius-cut RBS are shown in Figs. 1 and 2. The grade of steel for the beams was SS400 with a specified minimum yield strength of 235 Mpa

TABLE 1 Test specimens

Specimen	Beam and column	Panel zone strength	Beam web connection method	<i>a</i> (mm)	<i>b</i> (mm)	<i>c</i> (mm)	Flange reduction (%)
Set No. 1							
DB700-SW	H700X300X13X24 (SS400) H428X407X20X35 (SM490)	Strong (10 mm doubler plate, SM490)	Welded	175	525	55	37
DB700-MW	H700X300X13X24 (SS400) H428X407X20X35 (SM490)	Medium	Welded	175	525	55	37
DB700-SB	H700X300X13X24 (SS400) H428X407X20X35 (SM490)	Strong (10 mm doubler plate, SM490)	Bolted	175	525	55	37
DB700-MB	H700X300X13X24 (SS400) H428X407X20X35 (SM490)	Medium	Bolted	175	525	55	37
Set No. 2							
DB600-MW1	H600X200X11X17 (SS400) H400X400X13X21 (SM490)	Medium	Welded	150	510	40	40
DB600-MW2	H600X200X11X17 (SS400) H400X400X13X21 (SM490)	Medium	Welded	150	390	40	40
DB600-SW1	H600X200X11X17 (SS400) H588X300X12X20 (SM490)	Strong	Welded	150	450	40	40
DB600-SW2	H606X201X12X20 (SS400) H588X300X12X20 (SM490)	Strong	Welded	150	450	40	40

(34 ksi); SM490 steel was used for the columns and the specified minimum yield strength was 324 Mpa (47 ksi). The tensile coupon test results are summarized in Table 2. The RBS design followed the

recommendations by Iwankiw (1997) and Engelhardt et al. (1998). The beam end length (a) and the total length of the RBS zone (b) were chosen as 25% and 75% of the beam depth, respectively. These dimensions were selected to minimize the reduction in flange area. The resulting distance from the centerline of the RBS to the column face was 62.5% of the beam depth. The strain hardened plastic moment at the RBS hinge was calculated using the expected yield strength of the beam ($F_{ye} = 313$ Mpa) and a strain hardening factor of 1.1.

TABLE 2. Tensile coupon test results

Member	Coupon	Yield strength (MPa)	Tensile strength (MPa)	Yield ratio (%)
Beam H700X300X13X24 (SS400)	Flange	304	455	67
	Web	364	480	76
Column H428X407X20X35 (SM490)	Flange	343	512	67
	Web	358	520	69
Beam H600X200X11X17 (SS400)	Flange	326	467	70
	Web	343	473	73
Column H400X400X13X21 (SM490)	Flange	358	525	68
	Web	374	531	74
Beam H606X201X12X20 (SS400)	Flange	295	447	66
	Web	333	471	71
Column H588X300X12X20 (SM490)	Flange	374	534	70
	Web	405	546	74

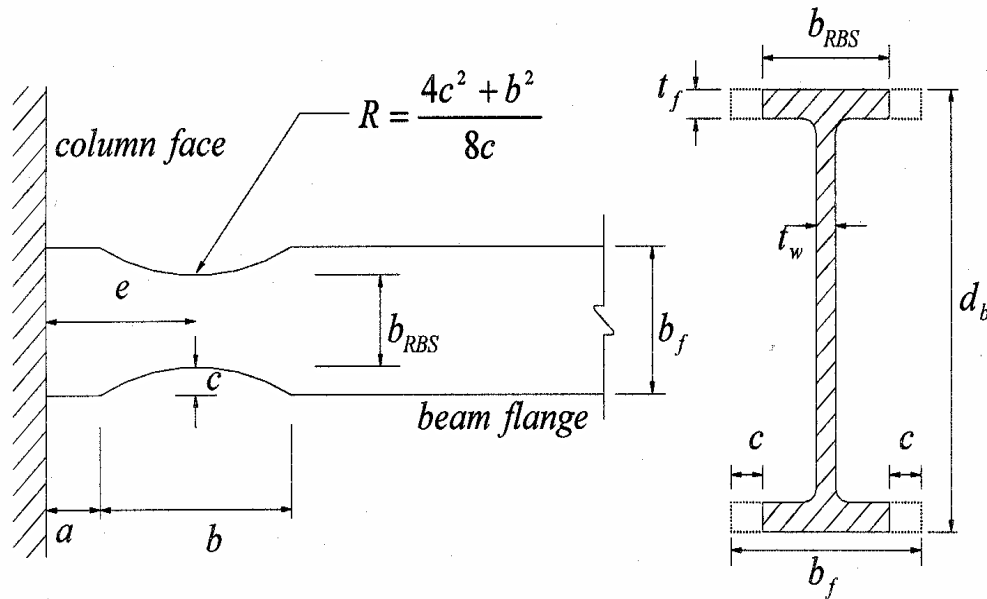


Fig. 1 Typical geometry of the radius-cut RBS

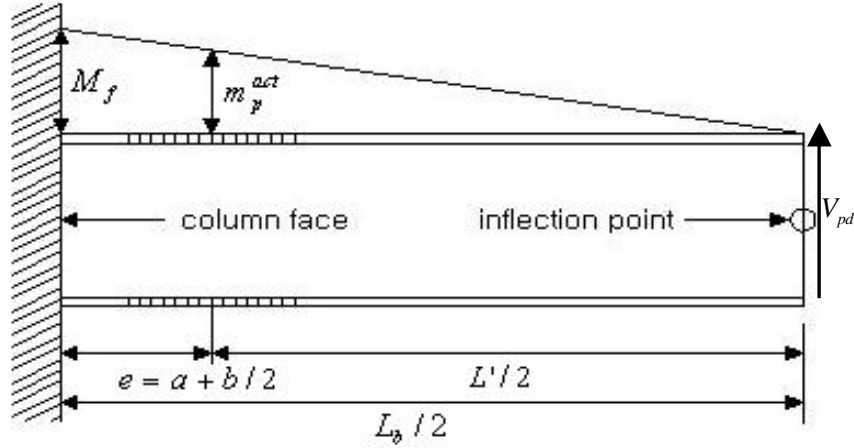


Fig. 2 Seismic moment profile for RBS design

$$m_p^{act} = \alpha \times Z_{RBS} \times F_{ye} = (1.1) \times Z_{RBS} \times F_{ye} \quad (1)$$

Engelhardt et al. (1998) recommended that the moment at the face of the column be limited to approximately 85 to 100 percent of M_p , where M_p = expected plastic moment of the beam. In this study the trimmed flanges were sized to limit the moment at the column face to about 90 percent of M_p as follows.

$$0.90 \times M_p \geq M_f = m_p^{act} \times \left(\frac{L_b}{L} \right) \quad (2)$$

The reduction in flange area at the RBS center was 37% and 40% for Set No. 1 and Set No. 2, respectively (see Table 1). The flange reduction in Set No. 1 was slightly less than the 40% minimum reduction limit of the SAC recommendation (SAC 2000). The panel zones were then designed by using either of the following two equations for the panel zone design strength:

$$V_p = (0.75)(0.6F_{yc}d_c t_p) \left[1 + \frac{3b_{cf}t_{cf}^2}{d_b d_c t_p} \right] \quad (3)$$

$$V_p = (0.6F_{yc}d_c t_p) \left[1 + \frac{3b_{cf}t_{cf}^2}{d_b d_c t_p} \right] \quad (4)$$

where F_{yc} = yield strength of the column web, d_b = beam depth, d_c = the column depth, t_p = thickness of the panel zone, b_{cf} = the column flange width, and t_{cf} = the column flange thickness. Eq. (3) was implemented in the AISC Seismic Provision (AISC 1997). Specimens with panel zone designed by Eq. (3) are defined as strong panel zone specimens in this study. In Set No. 1, nominally identical steel shapes were used for the beams and columns, respectively. When Eq. (3) was used for the panel zone strength, doubler plates of 10 mm thickness were provided to specimens DB700-SB and DB700-SW. The doubler plates were plug-welded to the column web to prevent premature local buckling under large cyclic inelastic shear deformations (AISC 1997, AWS 2000). Eq. (4), which is adopted in the 2002 AISC Seismic Provisions, was used to design medium panel zone specimens. This equation, which does not include the resistance factor (0.75), represents the panel zone shear strength at 4 times the shear strain at yield (Krawinkler

1978). Four medium panel zone specimens were included in this testing program (DB700-MW and DB700-MB in Set No. 1, DB600-MW1 and DB600-MW2 in Set No. 2). Specimens DB600-MW1 and DB600-MW2 in Set No. 2 were identical except for a slight difference in the RBS length: that is, the RBS length was taken as 85% (DB600-MW1) and 65% (DB600-MW2) of the beam depth.

Most of the past tests have been conducted on specimens with a fully welded beam web. Recently, Jones et al. (2002) indicated that the use of a welded web connection does provide some benefit to the connection performance and it tends to reduce the vulnerability of the connection to weld fracture. To further investigate the influence of the beam web connection, two bolted web specimens, DB700-SB and DB700-MB, were included in Set No. 1. With a slip coefficient of 0.33, the slip-critical bolted web connection consisted of eight fully tensioned-M22-F10T high strength bolts. The bolts were tightened with the calibrated wrench method with a specified tension level of 201 kN. The ultimate strength of the bolted web connection was about two times the expected maximum beam shear. In Set No. 2, all the beam webs were groove-welded to the column flange. Continuity plates equal in thickness to the beam flange were provided in all specimens. Electrodes with a specified minimum Charpy V-Notch (CVN) toughness of 26.7 Joule at -28.9°C (20 ft-lb at -20°F) was specified for flux-cored arc welding. Weld access hole configurations followed the SAC recommendations (SAC 2000). Fig. 3 shows the connection details for specimen DB700-SB. In Table 1, the following abbreviations were used for the specimen designation: S= strong panel zone, M= medium panel zone, W= welded web, and B= bolted web.

Test setup and Loading

The specimens were mounted to a strong floor and a strong wall. An overall view of the test setup is shown in Fig. 4. Lateral restraint was provided at a distance of 2500 mm from the column face. The specimens were tested statically according to the SAC standard loading protocol (Krawinkler et al. 2000). The beam tip displacement corresponding to 1% story drift ratio was 38 mm. The test specimens were instrumented with a combination of displacement transducers and strain gages to measure global and local responses. Whitewash was painted in the connection region to monitor yielding

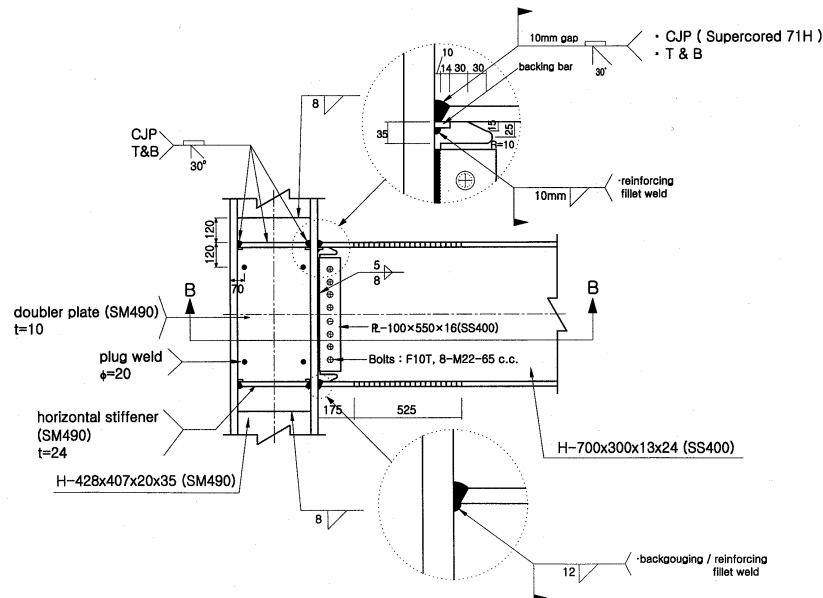


Fig. 3 Specimen DB700-SB moment connection details

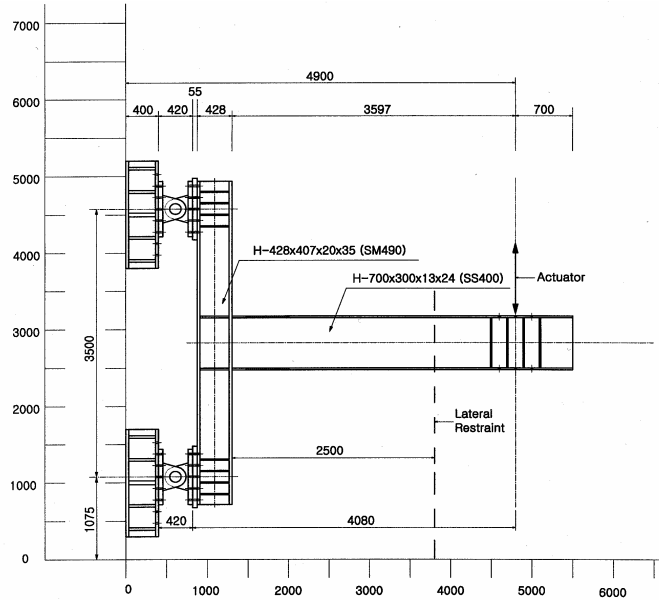


Fig. 4 Test setup

TEST RESULT AND DISCUSSION

The cyclic responses of the specimens in Set No. 1 are presented in Fig. 5. The ordinate is expressed in terms of the normalized moment at the column face; the normalization was based on the nominal plastic moment of the original (unreduced) beam section. Both strong and medium panel zone specimens with a welded web connection developed satisfactory levels of ductility required for special moment frames.

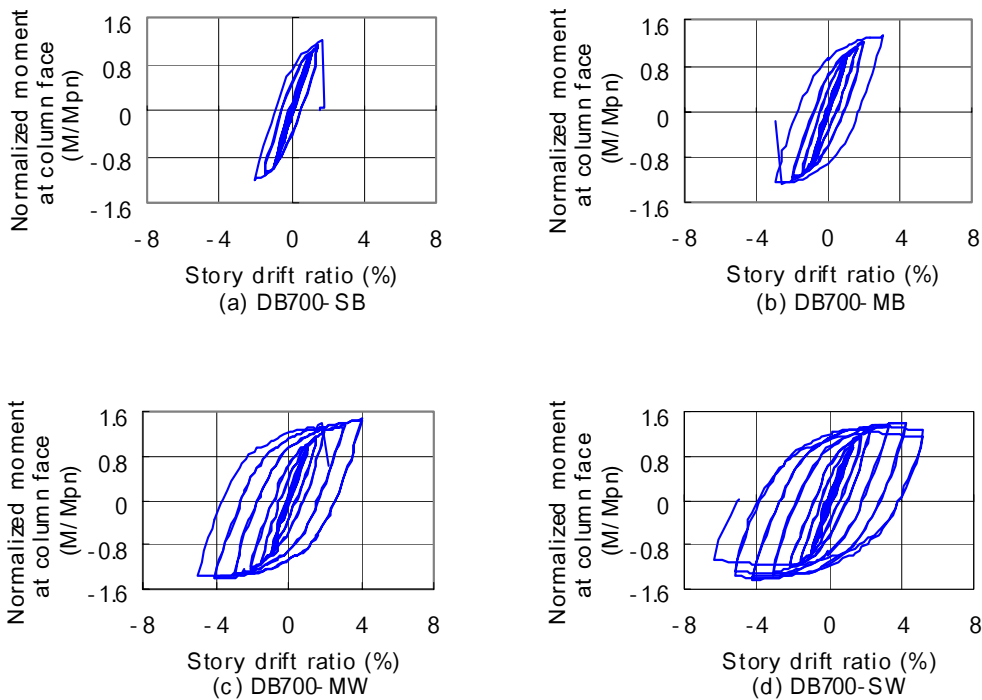


Fig. 5 Normalized moment versus story drift ratio relationship (Set No.1)

But specimens with a bolted web connection performed poorly due to premature brittle fracture of the beam flange at the weld access hole (see Fig. 6). A complete fracture across the beam flange width was developed in both cases. Fig. 7 shows the plastic hinge formation in the welded web specimens. Significant yielding of the panel zone in specimen DB700-MW was evident from the flaking of the whitewash. Specimen DB700-SW exhibited excellent connection rotation capacity up to 6% story drift without fracture.



Fig.6 Beam bottom flange fracture of specimen DB700-SB at 2% story drift



Fig. 7 Connection region of specimens DB700-MW and DB700-SW

Fig. 8 shows a comparison of the normalized maximum moment at the centerline of the RBS (i.e., assumed plastic hinge location). The normalization was based on the actual plastic moment of the narrowest reduced beam section. At a given story drift ratio, the figure shows that the bolted web specimens were less efficient in developing moment capacity. Tsai and Popov (1988) indicated that web bolts typically slip during testing, leaving the welded flanges alone to resist the total moment. Fig. 9 compares the cyclic flexural strain responses of specimens DB700-SB and DB700-SW near the groove weld of the beam bottom flange up to the fracture point of specimen DB700-SB. Much higher strain demand on the bolted web specimen is evident. These measured results appear to be consistent with the observation by Tsai and Popov. Goel et al. (1997) pointed out that the area in the middle of the beam web near the shear tab is virtually devoid of stresses and much of the shear force is transferred through the beam flanges, thus leading to overstressing of the beam flanges. The measured cyclic shear strain responses are presented in Fig. 10. These measured results support the foregoing observations by Goel et al. Reverse shear occurs in the middle of the beam web. This is undesirable because reverse shear will increase the shear demand in other part of the connection to meet the force equilibrium. The shear transfer mechanism in the RBS connection is still not consistent with that predicted by the classical beam theory and should be reexamined more thoroughly. It appears that the high incidence of base metal fracture in specimens with bolted web connections is related to, at least in part, the increased demand due to the web

bolt slippage and actual load transfer mechanism significantly different from that usually assumed in connection design. Plastic straining of the beam flange can lead to a redistribution of shear stress. However, considering that the plastic straining would concentrate in the RBS region, the shear stress redistribution approaching that of the beam theory seems difficult to occur near the column face.

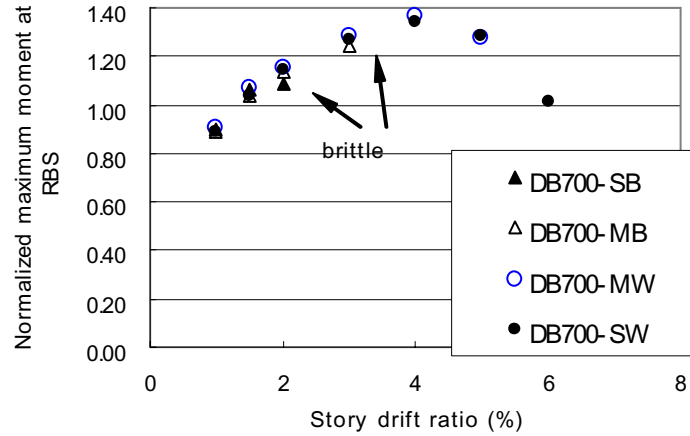


Fig. 8 Comparison of normalized maximum moment at RBS (Set No. 1)

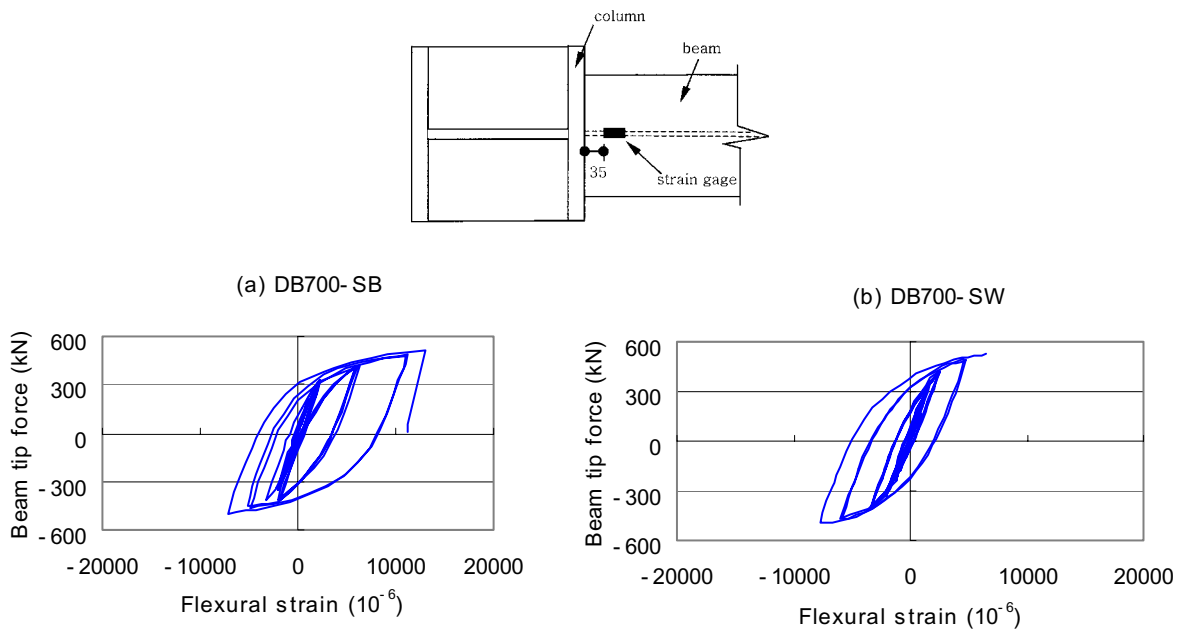


Fig. 9 Comparison of measured flexural strain responses near the groove weld

The plots shown in Fig. 11 indicate that all specimens in Set No. 2, with both strong and medium panel strengths, exhibited satisfactory connection ductility. Fig. 12 presents a comparison of the lateral-torsional buckling (LTB) amplitudes measured up to the 4% story drift cycles. Because both the beam and the panel zone contributed to plastic rotation in the medium panel zone specimens, LTB amplitudes were reduced. This is a sure advantage to reducing the tendency for global instability of the RBS beam. The cyclic strain hardening factor computed at the RBS center based on the measured yield strength of the beam was of

similar magnitude between the medium and strong panel zone specimens, and reached an average value of 1.27 at 4% story drift. This value is higher than that usually assumed (1.1) in design (AISC 2000).

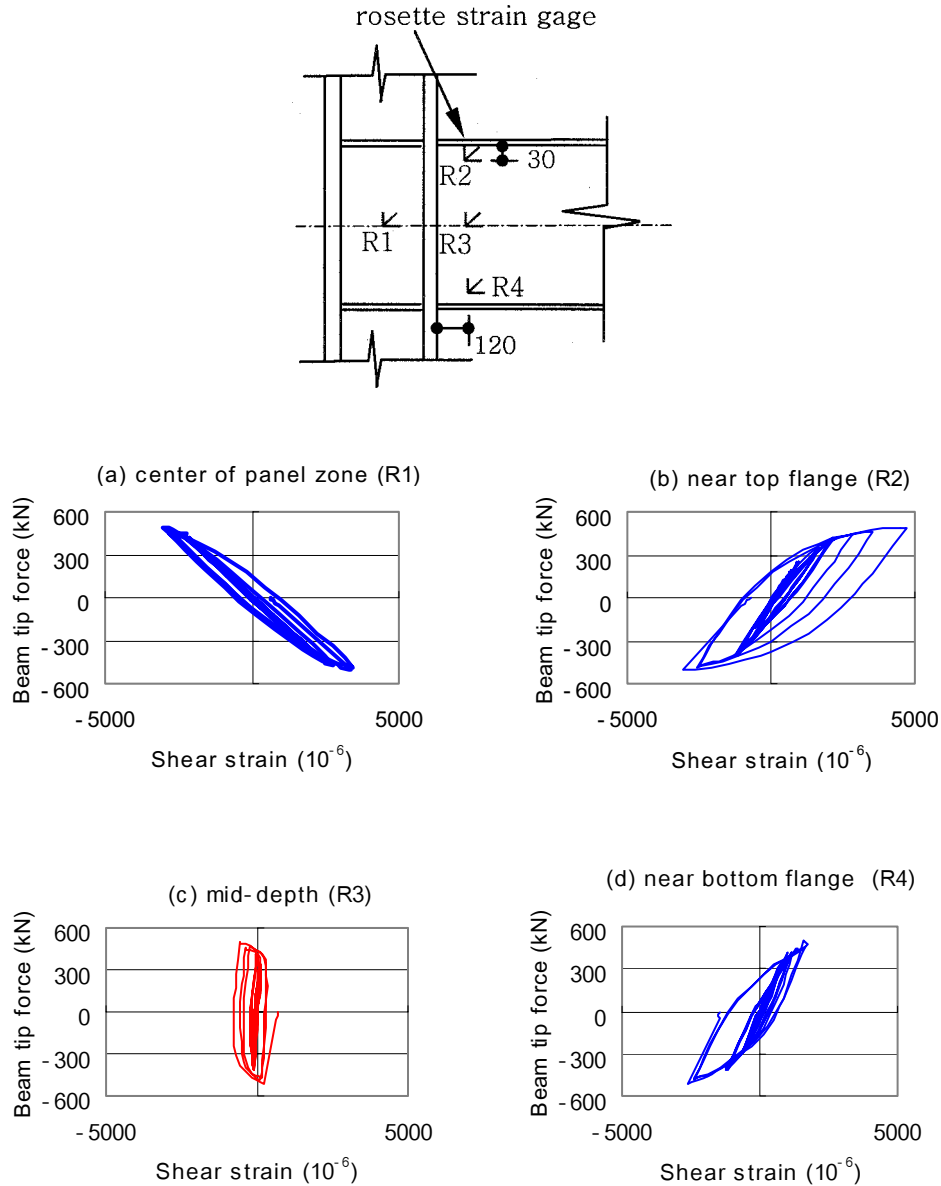


Fig. 10 Measured cyclic shear strain responses (specimen DB700-SB)

Effects of panel zone strength on some connection responses are summarized in Table 3. For the purpose of analyzing the effects of panel zone strength, two formulae were used as a measure of the panel zone strength in this study. The first one is based on the Von Mises yield criterion (Eq. 5),

$$V_y = \frac{1}{\sqrt{3}} F_{yc} d_c t_p \approx 0.6 F_{yc} d_c t_p \quad (5)$$

and the second one is based on the Krawinkler's recommendation (Eq. 4), which includes the contribution of the column flange to the post-yield strength. The measured yield strength in Table 2 was used to calculate the panel zone strength.

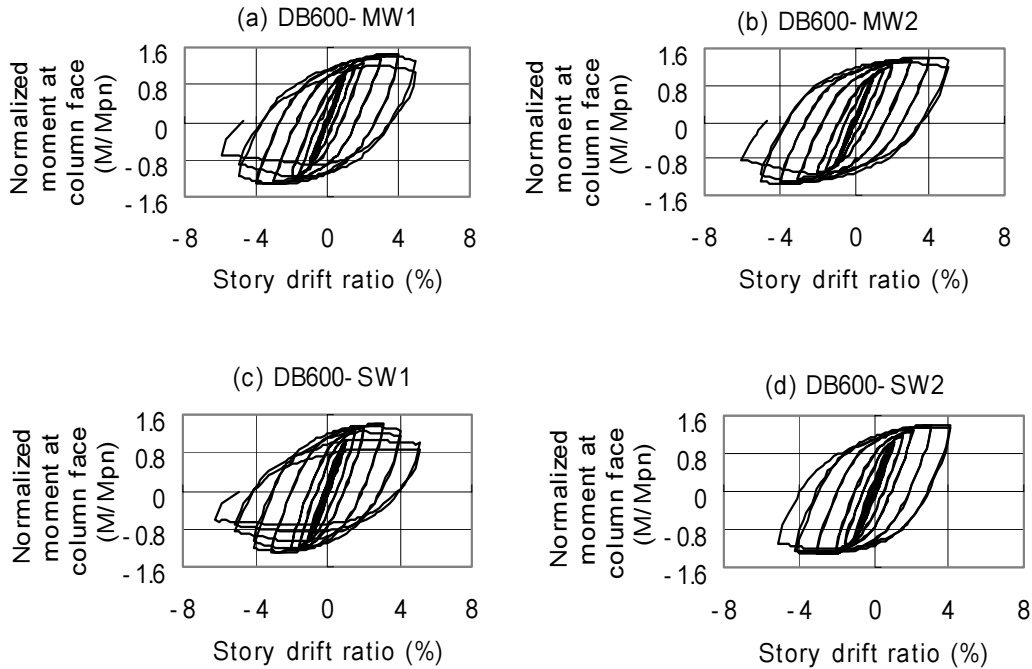


Fig. 11 Normalized moment versus story drift ratio relationship (Set No. 2)

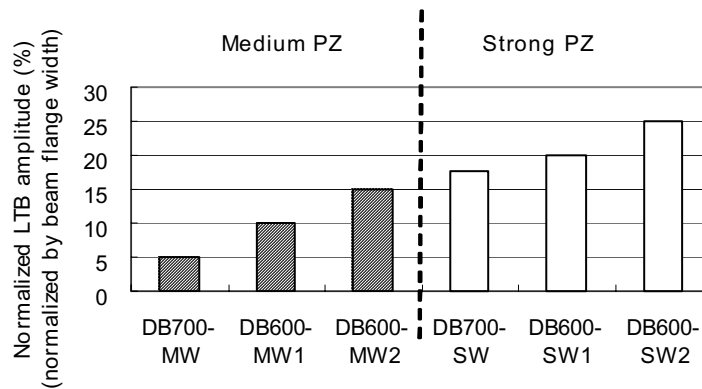


Fig. 12 Comparison of LTB amplitudes at 4% story drift cycle

As a measure of the beam strength, the panel zone shear force $V_{RBS, P}$ corresponding to the actual plastic moment of the RBS was used; a similar strength measure was used by Roeder (2002). For a one-sided moment connection, $V_{RBS, P}$ can be computed as follows:

$$V_{RBS,P} = \left(\frac{M_{RBS,P}}{d_b} \right) \times \left(\frac{L_b/2 + d_c/2}{L_b/2 - e} \right) \times \left(1 - \frac{d_b}{H_c} \right) \quad (6)$$

where $M_{RBS,P}$ = actual plastic moment at the RBS center based on the measured yield stress, H_c = column height, and refer to Fig. 2 for some remaining symbols. In Table 3, specimen DB700-SW was excluded because the tensile coupon test results for the doubler plates were not available. To augment the database, one test result from Chi and Uang (2002) was included. Since available test results show that the panel zone can easily develop a plastic rotation of 0.01 rad. without causing distress to the beam flange groove welds, and Table 3 shows that the panel zone at this deformation level would dissipate about 30% to 40% of the total energy, for a balanced design it is suggested that either of the following criterion be satisfied in design:

Table 3. Effects of panel zone strength on plastic rotation and energy dissipation

Specimen	PZ strength relative to beam		Panel zone plastic rotation at 4% story drift ratio (rad)	Energy dissipation by panel zone up to 4% story drift cycle (%)
	$V_{RBS,p}/V_y$	$V_{RBS,p}/V_p$		
DB700-MW	1.08	0.87	0.012	43
DB600-MW1	0.97	0.83	0.008	32
DB600-MW2	0.95	0.82	0.009	30
DC2*	0.74	0.67	0.005	24
DB600-SW1	0.71	0.66	0.0002	5
DB600-SW2	0.68	0.63	Negligible	Negligible

* From Chi and Uang (2002)

$$0.90 \leq \frac{V_{RBS,p}}{V_y} \leq 1.1 \quad (7)$$

or,

$$0.70 \leq \frac{V_{RBS,p}}{V_p} \leq 0.90 \quad (8)$$

This recommended range attempts to achieve the following:

- (1) to minimize the use of expensive doubler plates, which often require welding near the k area of the column,
- (2) to reduce the amount of beam buckling amplitude (i.e., beam torsion), and
- (3) to encourage the panel zone to provide about 0.01 rad. plastic rotation, which corresponds to about 30% to 40% of the total energy dissipation in the connection region.

CONCLUSIONS

The results of this study are summarized as follows.

- (1) Both strong and medium panel zone specimens with welded web connection exhibited satisfactory levels of connection ductility required of special moment-resisting frames. Specimens with a bolted web connection performed poorly due to premature brittle fracture of the beam flange at the weld access hole. If fracture within the beam flange groove weld in a bolted web connection was avoided by using quality

welding, fracture tended to move into the beam flange base metal at the weld access hole. The measured strain data appear to imply that the high incidence of base metal fracture in specimens with bolted web connections is related to, at least in part, the increased demand on the beam flanges due to the web bolt slippage and the actual load transfer mechanism which is completely different from that usually assumed in connection design.

(2) For welded-web RBS moment connections, test results showed that the panel zone could easily developed a plastic rotation of 0.01 rad. without distressing the beam flange groove welds. With this level of inelastic deformation, the panel zone would dissipate about 30% to 40% of the energy. Allowing the panel zone to deform inelastically at this level also reduces the magnitude of beam distortion (e.g., lateral torsional buckling) by about a half. A criterion for a balanced PZ strength that improves the plastic rotation capacity while reduces the amount of beam distortion is presented.

Acknowledgments

Funding for this research to the first author was provided by the Korea Earthquake Research Center (KEERC Project No. R11-1997-045-11004-0) and the Research Institute of Industrial Science and Technology (RIST) in Korea.

REFERENCES

1. Chen, S. J., Yeh, C. H., and Chu, J. M. "Ductile steel beam-to-column connections for seismic resistance." *J. Struct. Engrg.*, ASCE, 122(11), 1996: 1292-1299.
2. Chi, B. and Uang, C.-M. "Cyclic response and design recommendations of reduced beam section moment connections with deep column." *J. Struct. Engrg.*, ASCE, 128(4), 2002: 464-473.
3. Engelhardt, M. D., Winneberger, T., Zekany, A. J., Potyraj, T. J. "Experimental investigations of dogbone moment connections." *Engrg. J.*, 35(4), AISC, Fourth Quarter, 1998: 128-139
4. Gilton, C. S. and Uang, C.-M. "Cyclic response and design recommendations of weak-axis reduced beam section moment connections." *J. Struct. Engrg.*, ASCE, 128(4), 2002: 452-463
5. Goel, S. C., Stojadinovic, B., and Lee, H.-K. "Truss analogy for steel moment connections", *Eng. J.* 34(2), 1997: 43-53.
6. Iwankiw, N. "Ultimate strength consideration for seismic design of the reduced beam section (internal plastic hinge)." *Engrg. J.* 34(1), 1997: 3-16.
7. Jones, S. L., Fry, G. T., and Engelhardt, M. D. "Experimental evaluation of cyclically loaded reduced beam section moment connections." *J. Struct. Engrg.*, ASCE, 128(4), 2002: 441-451.
8. Krawinkler, H. "Shear in beam-column joints in seismic design of steel frames." *Engrg. J.* 15(3), 1978: 82-91
9. Krawinkler, H., Gupta, A., Medina, R., and Ruco, N. "Loading histories for seismic performance testing of SMRF components and assemblies." *Report No. SAC/BD-00/10*. SAC Joint Venture, Sacramento, Calif., 2000.
10. Plumier, A "The dogbone: back to the future." *Engrg. J.* 34(2), 1997: 61-67

11. Roeder, C. W. "General issues influencing connection performance." *J. Struct. Engrg.*, ASCE, 128(4), 2002: 420-428.
12. SAC. "Seismic design criteria for new moment-resisting steel frame construction." *Report No. FEMA 350*, SAC Joint Venture, Sacramento, Calif., 2000.
13. American Institute of Steel Construction (AISC). *Seismic provisions for structural steel buildings.*, American Institute of Steel Construction, Chicago, 1997 and 2000.
14. American Welding Society (AWS). *Structural welding code-steel*, AWS D1.1: Section 3.10, American Welding Society, FL., 2000.
15. Tsai, K. C. and Popov, E. P. "Steel beam-column joints in seismic moment resisting frames." *EERC Report, UCB/EERC-88/19*, Univ. of California, Berkeley, 1988.
16. Zekioglu, A., Mozaffarian, H., Chang, K. L., and Uang, C.-M. "Designing after Northridge." *Modern Steel Constr.*, 37(3), 1997: 36-42.